Magnetic Field versus Temperature Phase Diagram of a Quasi-One-Dimensional $S = 1$ Heisenberg Antiferromagnet

Z. Honda,* H. Asakawa, and K. Katsumata

The Institute of Physical and Chemical Research (RIKEN), Wako, Saitama 351-0198, Japan

(Received 15 April 1998)

From a heat capacity (C_p) measurement on a single crystal sample of the $S = 1$ quasi-one-dimensional (Q1D) Heisenberg antiferromagnet (HAF) $Ni(C_5H_{14}N_2)_2N_3(PF_6)$ in applied magnetic fields, we found an anomaly which is indicative of a magnetic long-range ordering. We were able to follow how the position of the anomaly in C_p changes with temperature (T) and magnetic field (H). An experimental H-T phase diagram of an $S = 1$ Q1D HAF is obtained and compared with that of the corresponding classical system. [S0031-9007(98)07105-1]

PACS numbers: 75.30.Kz, 75.10.Jm, 75.40.Cx, 75.50.Ee

Although the theoretical study of one-dimensional (1D) magnetism began in the 1930s [1], several decades passed before suitable model compounds became available [2]. Quasi-1D magnets, in which the magnetic interaction in one direction dominates, with much weaker interactions in other directions, exhibit a short-range ordering over a wide temperature range and usually show a long-range ordering (LRO) at finite temperature due to the interchain coupling (J'). The situation is largely altered in the case of quasi-1D Heisenberg antiferromagnet (HAF) with integer spin quantum number (S). As has been predicted by Haldane [3], there is an energy gap (Haldane gap) between the singlet ground state and first excited triplet in an $S = 1$ 1D HAF. The effects of J' on the Haldane gap have been studied theoretically [4,5] and the results show that the Haldane gap survives even at $T = 0$ K, if J' is small [$(z'J'/J \lesssim 0.05)$ z': number of adjacent chains; J: intrachain coupling]. Therefore, quasi-1D $S = 1$ HAF compounds with small J' become nonmagnetic at low temperatures and no LRO occurs. On the other hand, strong magnetic fields destroy the Haldane gap and the system recovers magnetism [6]. Then, we expect a magnetic ordering to occur in a quasi-1D $S = 1$ HAF under high fields and at low temperatures.

The magnetic ordering in a quasi-1D classical HAF has been studied both theoretically [7,8] and experimentally [9,10]. These experiments showed that the Néel temperature (T_N) of the quasi-1D $S = 5/2$ HAF compound $(CH_3)_4NMnCl_3$ (TMMC) which exists already in zero field increases with increasing field.

In a previous paper [11], we reported experimental evidence for the field induced magnetic ordering in the $S = 1$ quasi-1D HAF compound $Ni(C_5H_{14}N_2)_2N_3(ClO_4)$, abbreviated NDMAZ. From a heat capacity (C_p) measurement on a single crystal sample of NDMAZ, we observed an anomaly at about 0.6 K and at 12 T which indicated that a magnetic ordering occurred there. Because of limitations in our calorimeter, we were unable to follow how the position of the anomaly in C_p changes with temperature (T) and magnetic field (H). We then tried to synthesize a new quasi-1D HAF compound with a weaker intrachain exchange interaction in which an LRO is expected to be induced at a lower field. In this paper, we report the first experimental H-T phase diagram of a quasi-1D $S = 1$ HAF which might be interesting to broad audiences. It is also interesting to compare the H-T phase diagram of the quantum system with that of the classical one.

The compound we are studying here is $Ni(C_5H_{14}N_2)_2N_3(PF_6)$ [12], abbreviated NDMAP. If one replaces ClO_4 counteranion in NDMAZ by PF_6, one gets NDMAP. Therefore, the crystal and magnetic properties of NDMAZ and NDMAP are very similar. The powder samples of NDMAP were synthesized by a similar method reported in [12]. The single crystals of NDMAP were grown from an aqueous solution of the powder samples.

Figure 1 shows the temperature dependence of the susceptibility of a single crystal of NDMAP measured with a SQUID magnetometer (Quantum Design MPMS2). We see that a broad peak appears at about 30 K and

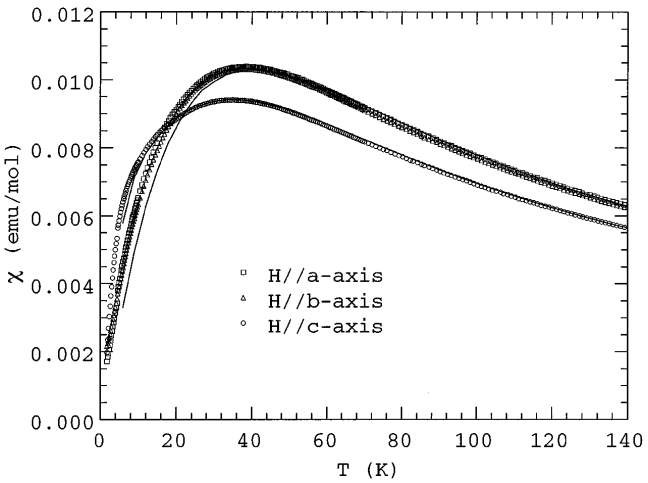

FIG. 1. Temperature dependence of the magnetic susceptibility of a single crystal sample of NDMAP measured at 0.01 T. Full curves are the theoretical ones discussed in the text.

 0031-9007/98/81(12)/2566(4)$15.00

that the susceptibility decreases steeply for all of the crystal axes when the temperature is decreased further. This behavior of magnetic susceptibility is characteristic of an $S = 1$ 1D HAF system. There is an anisotropy in the susceptibility which can be explained as due to the single-ion anisotropy of Ni^{2+}. We have compared the experimental data with a theory obtained by the quantum transfer matrix method. The Hamiltonian we used is expressed as

$$\mathcal{H} = J \sum_i \mathbf{S}_i \cdot \mathbf{S}_{i+1} + D \sum_i (S_i^z)^2 - \mu_B \sum_i \mathbf{S}_i \cdot \tilde{g} \cdot \mathbf{H}, \quad (1)$$

where D is the single-ion anisotropy constant, μ_B is the Bohr magneton, and $\tilde{g}$ is the g tensor. In this calculation, we neglected J', because the effect of it on the susceptibility should be small at high temperatures. From the comparison between theory and experiment, we get the following values:

$$J/k_B = 30.0 \text{ K}, \qquad D/J = 0.3,$$

$$g_{\parallel} = 2.10, \quad \text{and} \quad g_{\perp} = 2.17.$$

Here, $g_{\parallel}$ and $g_{\perp}$ are the g values parallel and perpendicular to the chain c axis, respectively. The values of J in NDMAP is almost half of that in NDMAZ.

We have measured the heat capacity of a single crystal of NDMAP using a Mag Lab^{HC} microcalorimeter (Oxford Instruments, UK). Figure 2 shows the temperature dependence of the total heat capacity, including the contribution of the lattice measured in applied magnetic field parallel to the chain c axis. We see no anomaly in C_p in zero field down to 0.6 K as expected. With increasing field, we clearly see an anomaly. The position of the anomaly does not depend much on H in this direction.

We show in Fig. 3 the results obtained when H is applied perpendicular to the chain c axis. We see again an anomaly in C_p in finite H, the position of which moves to the high temperature side with increasing H. The heat capacity at high temperatures depends largely on H in this direction compared with that in the other direction (Fig. 2). Below 6 T, C_p does not depend much on H. On the other hand, C_p increases rapidly with H above 6 T. The heat capacity of a quasi-1D $S = 1$ HAF shows a broad peak near the temperature at which the susceptibility is a maximum (Fig. 1). The temperature (T_p), where C_p shows the broad peak, decreases with increasing H. The temperature range we are measuring in Figs. 2 and 3 is much lower than T_p and so we are observing the low temperature tail of the C_p curve. Note that the data presented in Figs. 2 and 3 contain the contribution of the lattice which is independent of H. In low fields, T_p is much higher than the temperature range we measured, so the tail does not change much with H. On the other hand, at high fields T_p decreases largely with H and the tail part grows nonlinearly with H. The different behavior of C_p for different directions (Figs. 2 and 3) reflects the different field dependence of the energy levels [6]. Details will be discussed elsewhere.

We have plotted in Fig. 4 the position of the anomaly obtained in the C_p measurements in the H-T plane. The low-T and low-H region below the boundary corresponds to the Haldane disordered phase, while the region above the boundary represents the LRO phase in its respective

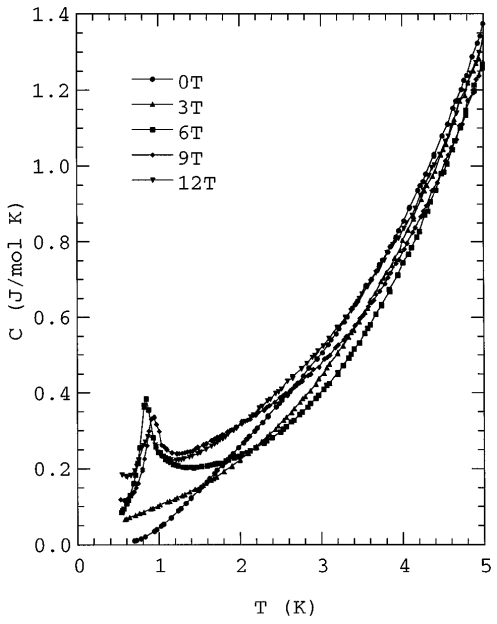

FIG. 2. Temperature dependence of the total heat capacity of a single crystal sample of NDMAP measured at the designated fields parallel to the c axis.

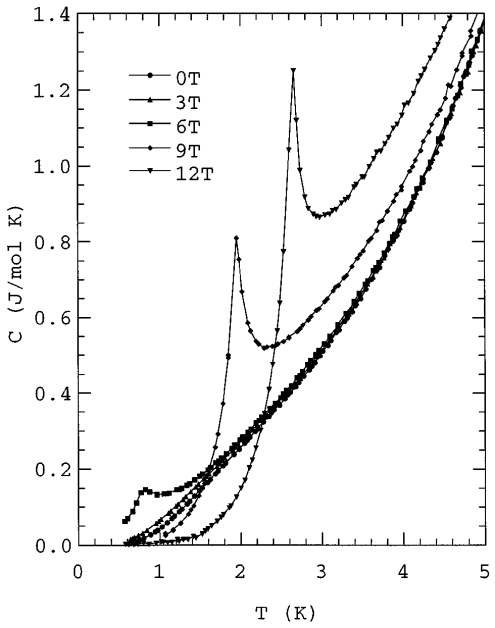

FIG. 3. Temperature dependence of the total heat capacity of a single crystal of NDMAP measured at different fields applied perpendicularly to the c axis.

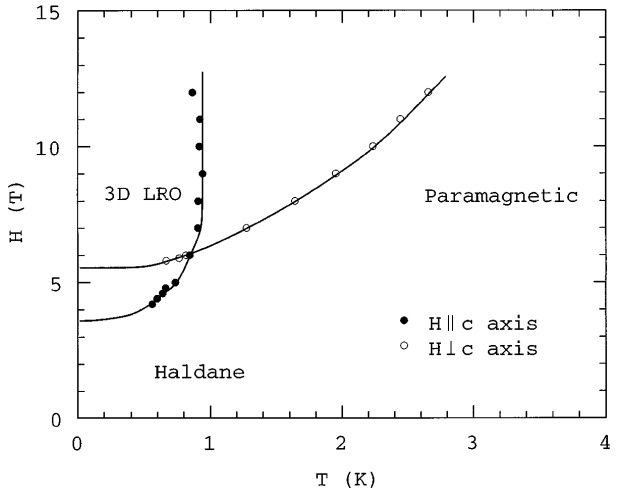

FIG. 4. Magnetic field versus temperature phase diagram of NDMAP obtained from the heat capacity measurements. Lines are guides to the eye.

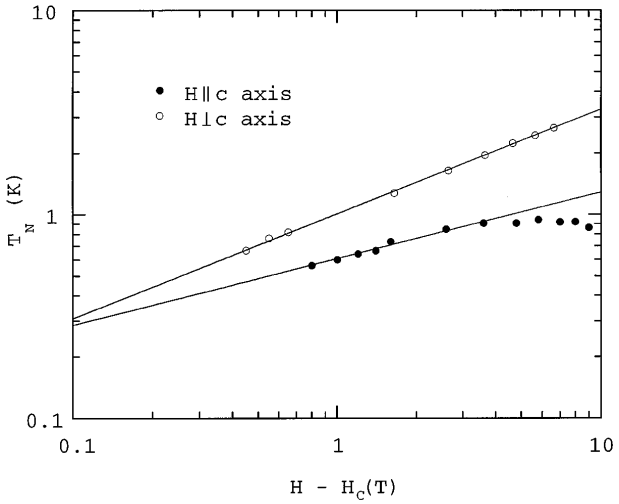

FIG. 5. The magnetic field dependence of the Néel temperature in NDMAP is plotted on a log-log scale.

field direction. There is an anisotropy in the phase boundary. The transition temperature from the paramagnetic to the LRO phase for a given H is higher for $H \perp c$ than that for $H \parallel c$ above about 6 T. Below 6 T, the situation is reversed.

This behavior is explained qualitatively as follows. Because the sign of the single-ion anisotropy constant (D) is positive, spins lie in a plane perpendicular to the c axis (the quantization axis of D is taken parallel to the c axis). When H is applied parallel to the c axis, the XY symmetry is retained. On the other hand, when H is applied perpendicularly to the c axis, the XY symmetry is broken and an Ising anisotropy is produced. It is widely accepted that the phase transition temperature of an Ising system is higher than that of an XY system for a given space dimensionality. This explains qualitatively what has been observed above about 6 T (Fig. 4). Because the critical field for $H \parallel$ chain is lower than that for $H \perp$ chain [6], we expect a crossing of the two phase boundary curves to occur at finite H and T, as observed (Fig. 4).

We plot in Fig. 5 the magnetic field dependence of T_N. Here the magnetic field is measured relative to the respective critical field ($H_{c\parallel}, H_{c\perp}$). Note that T_N exists only for $H > H_{c\parallel}$ or $H > H_{c\perp}$. We found that $T_N^{\perp}(H \perp c)$ varies as $T_N^{\perp} = A^{\perp}(H - H_c^{\perp})^{\phi_{\perp}}$, with $A^{\perp} = 1.006$ and $\phi_{\perp} = 0.513$. The magnetic field dependence of $T_N^{\parallel}(H \parallel c)$ is also expressed by $T_N^{\parallel} = A^{\parallel}(H - H_c^{\parallel})^{\phi_{\parallel}}$, with $A^{\parallel} = 0.607$ and $\phi_{\parallel} = 0.326$ in the limited range of magnetic fields. In the quasi-1D classical HAF compound TMMC, T_N was found to increase with H as

$$T_N(H) - T_N(0) = AH^2, \tag{2}$$

where $T_N(0)$ is the Néel temperature in zero field and A is a constant [9]. The H^2 dependence of $T_N(H)$ has been explained as due to the fact that the correlation length increases quadratically in H in the spin-wave approximation [7]. As far as we are aware, no theory exists on the field dependence of T_N for the $S = 1$ quasi-1D HAF. We expect, however, that the change of the correlation length with H in the $S = 1$ quasi-1D HAF is slower than that of the corresponding classical system, because of the strong quantum fluctuations in the former system. As noted above, $T_N^{\parallel,\perp}(H)$ exist only for $H > H_{c\parallel,c\perp}$. Then, we have the following expressions for the field dependence of $T_N^{\parallel,\perp}$:

$$T_N^{\parallel,\perp}(H) = A^{\parallel,\perp}(H - H_c^{\parallel,\perp})^{\phi}, \tag{3}$$

in agreement with the experimental observation. In Eq. (3), ϕ should be smaller than 2 because of the reason mentioned above, which is consistent with the experiment.

Finally, we present additional experimental evidence for the existence of a 3D LRO phase in this compound at the low-T and high-H region. We have made an electron spin resonance (ESR) measurement [13] on a single crystal of NDMAP using a high-frequency–high-field spectrometer installed at RIKEN [14]. At $T = 1.7$ K and $H \perp c$ axis, we found ESR signals above 8 T which are not on the paramagnetic resonance line and are fitted with the antiferromagnetic resonance theory [15] in the flopped phase. Below 8 T, we also found ESR signals which are explained as being due to transitions within the excited triplet in the Haldane state. These results of the ESR measurements are consistent with the H-T phase diagram shown in Fig. 4.

In conclusion, from the C_p measurements on a single crystal sample of the $S = 1$ quasi-1D HAF compound NDMAP in H, we found an anomaly which is indicative of a magnetic LRO. We were able to follow how the position of the anomaly in C_p changes with T and H. An experimental H-T phase diagram of an $S = 1$ quasi-1D HAF is obtained for the first time. The change of T_N with H is slower in an $S = 1$ quasi-1D HAF than in

the corresponding classical system. Clearly, theoretical studies on this subject are needed.

This work was partially supported by a Grant-in-Aid for Scientific Research from the Japanese Ministry of Education, Science, Sports and Culture. Z. H. was supported by the Research Fellowships of the Japan Society for the Promotion of Science for Young Scientists. H. A. was supported by the Special Researcher's Basic Science Program (RIKEN). We have made numerical calculations using a vector parallel computer (Fjitsu VPP 500/28) installed at RIKEN.

*Also at Graduate School of Science and Engineering, Saitama University, Urawa, Saitama 338-8570, Japan.

[1] H. Bethe, Z. Phys. **71**, 205 (1931).
[2] For a review, see L. J. de Jongh and A. R. Miedema, Adv. Phys. **23**, 1 (1974).
[3] F. D. M. Haldane, Phys. Rev. Lett. **50**, 1153 (1983).
[4] I. Affleck, Phys. Rev. Lett. **62**, 474 (1989).
[5] T. Sakai and M. Takahashi, Phys. Rev. B **42**, 4537 (1990).
[6] K. Katsumata, H. Hori, T. Takeuchi, M. Date, A. Yamagishi, and J. P. Renard, Phys. Rev. Lett. **63**, 86 (1989).
[7] Y. Imry, P. Pincus, and D. Scalapino, Phys. Rev. B **12**, 1978 (1975).
[8] F. Borsa, J.-P. Boucher, and J. Villain, J. Appl. Phys. **49**, 1326 (1978).
[9] C. Dupas and J. P. Renard, Solid State Commun. **20**, 581 (1976).
[10] K. Takeda, T. Koike, T. Tonegawa, and I. Harada, J. Phys. Soc. Jpn. **48**, 1115 (1980).
[11] Z. Honda, K. Katsumata, H. Aruga Katori, K. Yamada, T. Ohishi, T. Manabe, and M. Yamashita, J. Phys. Condens. Matter **9**, L83 (1997); *ibid.* **9**, 3487 (1997).
[12] M. Momfort, J. Ribas, X. Solans, and M. F. Bardia, Inorg. Chem. **35**, 7633 (1996).
[13] Z. Honda, K. Katsumata, M. Hagiwara, and H. Yamaguchi (unpublished).
[14] M. Hagiwara, K. Katsumata, I. Yamada, and H. Suzuki, J. Phys. Condens. Matter **8**, 7349 (1996).
[15] T. Nagamiya, K. Yosida, and R. Kubo, Adv. Phys. **4**, 1 (1955).